Directivity Evaluation of an Artificial Defect in a Simulated Butt Joint by the Visualization Method

The directivity of ultrasonic waves is investigated

BY Y. H. NAM

ABSTRACT. Ultrasonic testing uses the directivity of the ultrasonic wave, which propagates in one direction. The directivity is expressed as the relationship between the propagate direction and its sound pressure. The directivity of an ultrasonic wave is related to the choice of probe arrangement, testing sensitivity and scanning pitch and correct measurement of defect size and location.

This article investigates the directivity of ultrasonic waves that are scattered from a slit defect located in the heat-affected zone (HAZ) of a simulated butt-joint weld using the visualization method.

The directivity of shear waves scattered from the slit defect varied according to probe direction (far defect, near defect) and probe position (forward movement, maximum echo position, backward movement). A difference of directivity of the reflection wave was shown to exist between the 2- and 4-MHz angle probes. In the case of the 2-MHz angle probe, the directivity of the reflection wave appeared sharper than that of the 4-MHz angle probe because of the relation of the wave length and defect size.

Introduction

For detecting and characterizing the defects in ultrasonic testing, it is important to know the directivity of ultrasonic waves emitted from angle probes and reflected from the defect. In ultrasonic testing, the directivity of ultrasonic waves is closely related to the testing sensitivity, the scanning pitch, the arrangement of probes and the defect size and location (Refs. 1–2).

Since the sound pressure field in solids cannot be measured directly, most studies on ultrasonic directivity have been carried out in the theoretical field assuming the continuous wave. However, standard ultrasonic testing uses a pulse of an elastic wave in a solid. The directivity of the probe is ordinarily measured by using a semi-cylindrical shape test block and electrodynamic sensor. In this method, directivity of wave propagation cannot be precisely measured, and there is no method able to measure the directivity of reflected waves at the defect (Refs. 3–9).

We have developed an ultrasonic wave visualization system based on the synthesized photoelastic method. The system has high sensitivity for ultrasonic wave visualization and measures the sound pressure distribution from the visualized ultrasonic waves quantitatively.

The purpose of this work is to measure the directivity of the ultrasonic waves using the visualization method. We measured the directivity of shear waves emitted from angle probes and the directivity change with direction and position of the probe using the slit defect located in the HAZ of a simulated butt joint made of Pyrex glass.

KEY WORDS

Butt Joint
Defect
Directivity
Heat-Affected Zone
Ultrasonic Testing
Visualization
Wave Length

Visualization System

The configuration of the ultrasonic visualization system used in this study is shown in Fig. 1. The system consists of a regular linear polariscope with a commercial stroboscopic light source and a digital image-processing system (Refs. 10–12). The trigger pulse actuating the stroboscope has a delay time relative to the trigger pulse of the ultrasonic flaw detector, and by varying this delay time an observer can change the position at which the pulsed ultrasound is stroboscopically frozen and imaged. A CCD camera is used to visualize the ultrasonic wave in a solid. The image is divided into 512 lines, and each line is divided into 512 parts. The brightness is converted into a video signal with 8-bit resolution. The amplitude (brightness) of the ultrasonic wave is represented in polar coordinates (r, θ), using the values of 128 and 256 in terms of a directivity mean of 0.25 and 0.5 V, respectively, in the visualized image.

Directivity Analysis

Figure 2 schematically illustrates the manner by which directivity is determined from the visualized sound pressure image. The center point of directivity was first located from the circular curvature of the visualized shear wave. Next, two circles were set, which have radii r_1 and r_2 from the center, to fix the examination range of sound pressure in θ direction. This is especially important for the directivity analysis of reflected shear waves from the defect because ultrasonic scattering from the defect produces many reflected waves, so it is necessary to discriminate the wave to be analyzed. The directivities of the waves were obtained from the relationship between the angle θ and the maximum sound pressure value on the line from r_1 to r_2 (Refs. 13–15).

Y. H. NAM is with the R & D Center, Hanjung, Ltd., Changwon, Korea.

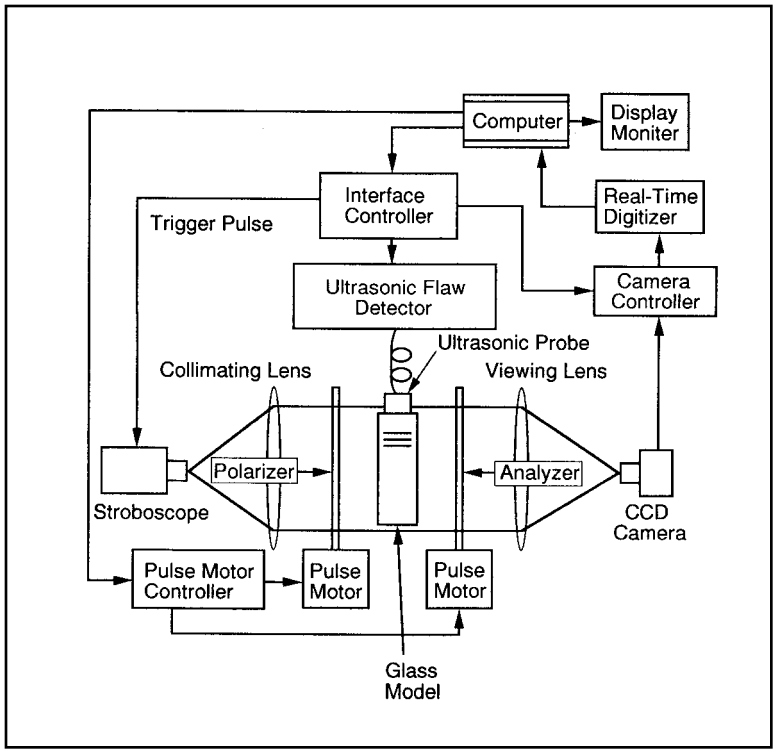

Fig.1 — Diagram of the sound pressure visualization system.

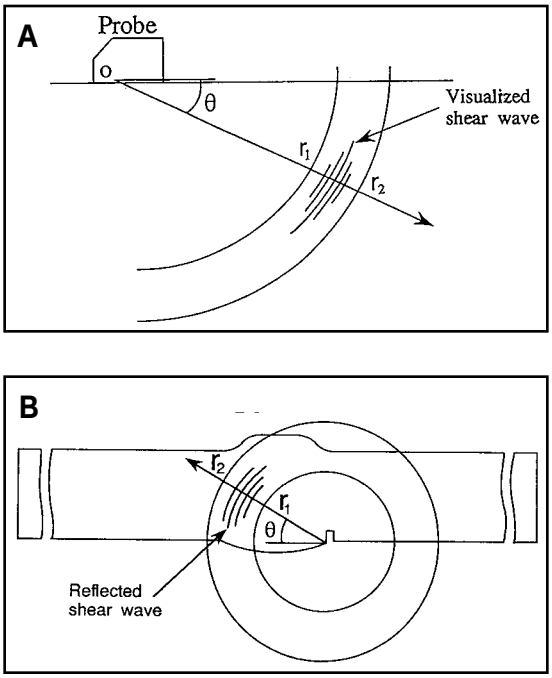

Fig. 2 — Determination of the directivity of ultrasonic waves: A — Shear wave emitted angle probe; B — shear waves reflected from defect.

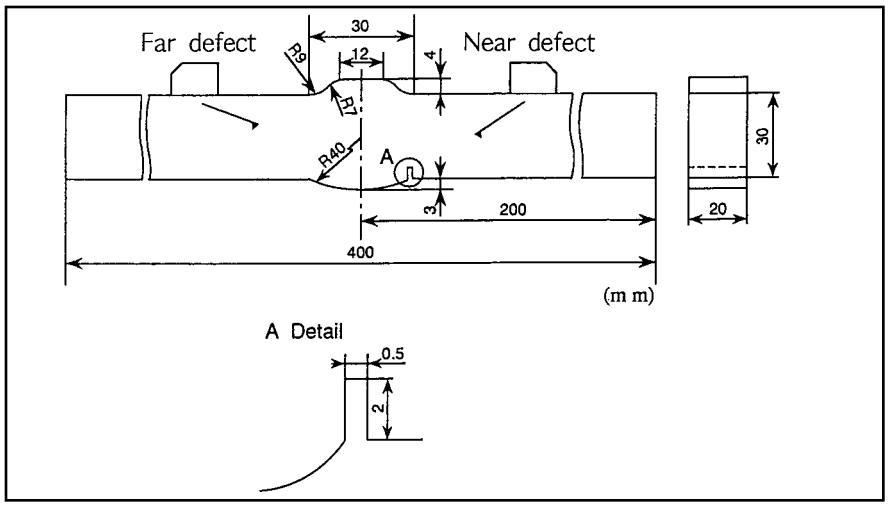

Fig. 3 — Dimension of the test specimen.

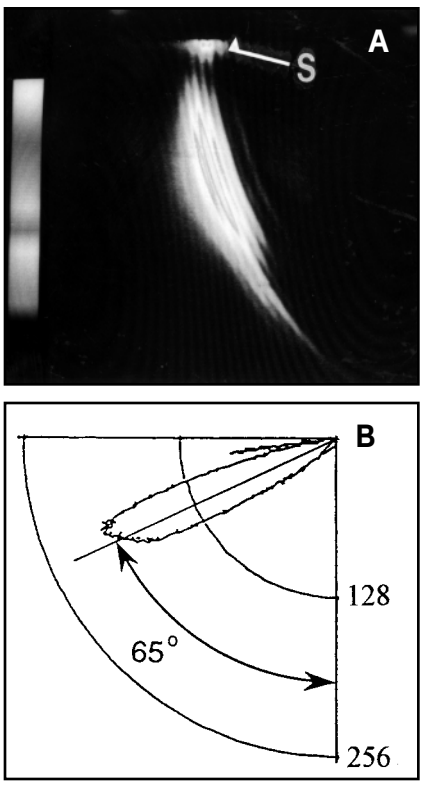

Fig. 4 — Directivity of 2-MHz, 60-deg angle probe: A — Visualization shear wave; B — directivity (R = 40 mm).

Experimental Method

Figure 3 shows the dimensions of the test specimens used in this experiment. Specimens made of Pyrex glass were used for ultrasonic visualization experiments because the glass has a better optical coefficient than inorganic glasses, small attenuation and a sound velocity (longitudinal wave: 5490 m/s, transverse wave: 3420 m/s) very similar to that of steel. A slit defect with a 2-mm depth was located in the HAZ in the simulated butt joint. Two angle probes were used with frequencies and nominal refraction angles for steel of 2 MHz, 60 deg and 4 MHz, 60 deg, respectively. The directivity of shear waves emitted from each angle probe were measured at four positions. The propagation distances (R) of the shear wave from the incident point of the angle probe are 40, 58, 76 and 94 mm. In the case of defect directivity, the reflected shear wave was set after 12- and

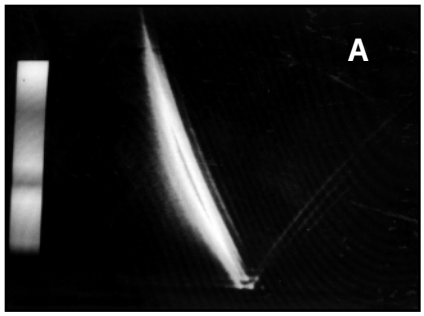

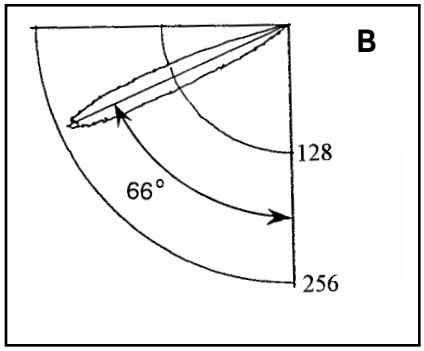

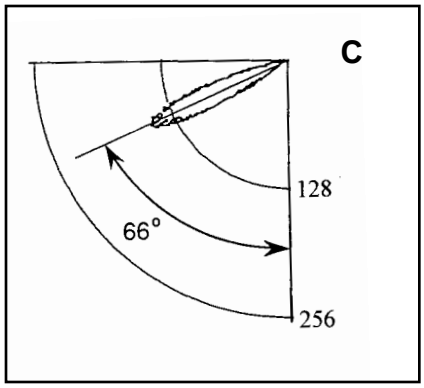

Fig. 5 — Directivity of 4-MHz, 60-deg angle probe: A — Visualization shear wave (R = 94 mm); B — directivity (R= 40 mm); C — directivity (R = 94 mm).

20-mm propagation from the slit root.

The directivity of the reflection wave was measured in two directions: far defect and near defect. Far defect means the angle probe is located left of the centerline in the simulated butt-joint weld; near defect means the angle probe is located right of the centerline — Fig. 3. The changes of directivity according to probe position are examined at three positions: forward movement, maximum echo position and backward movement. The maximum echo position means a probe was put at the maximum echo height position from the defect. The forward movement position means the probe was moved toward the defect from the maximum echo-height position to a position 6 dB less than the maximum. The backward movement position means the probe was moved away from the defect to a position 6 dB less than the maximum.

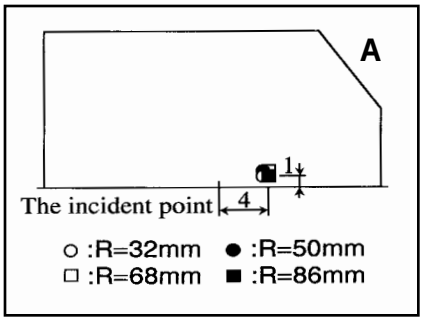

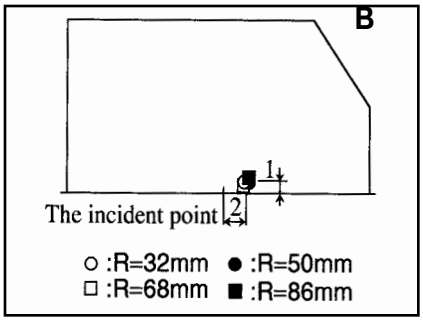

Fig. 6 —The center of directivity of angle probes: A — 2-MHz, 60-deg probe; B — 4-MHz, 60-deg probe.

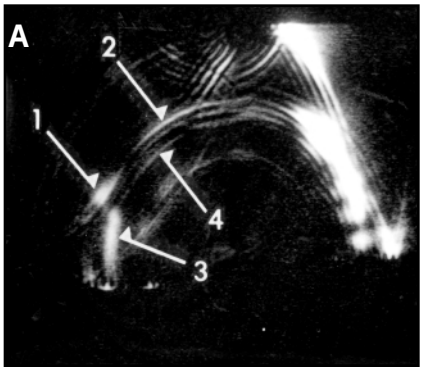

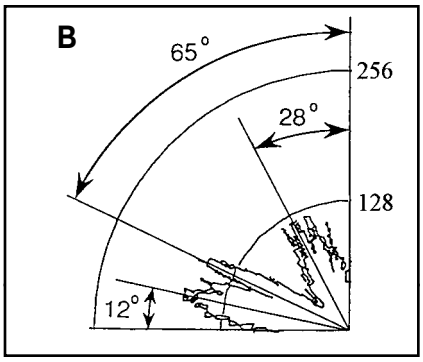

Fig. 7 — Directivity of 4-MHz, 60-deg shear waves reflected from far defect. (Probe was at the maximum echo position.) A — Visualized shear waves (R = 12 mm); B — directivity of reflected all-shear waves.

Results and Discussion

Directivity of Angle Probe

Figure 4A shows the visualization image of the shear wave emitted from the 2-MHz, 60 deg angle probe. The propagation distance R of the shear wave from the incident point of the probe was 40 mm. Sound pressure intensity is expressed by a 128 and 256 scale. Figure 4B presents the directivity obtained from Figure 4A. The directivity shown by the straight line shows surface wave (S) propagating along the surface of the test piece. The refracted angle of the 2-MHz angle probe was 65 deg in the glass specimen.

Figure 5A shows the visualization image of the shear wave emitted from the 4-MHz, 60-deg angle probe. Figure 5B presents the directivity, and the propagation distance of shear wave was 40 mm. The refracted angle of the 4-MHz shear waves was 66 deg. The directivity of the shear wave in the 2-MHz angle probe was wider than that of the 4-MHz angle probe. Figure 5C presents the directivity

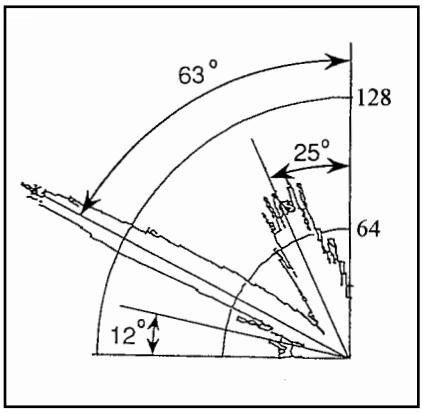

Fig. 8 — Change of directivity by probe forward movement (4 MHz, 60 deg).

obtained from Fig. 5A. The propagation distance R of the shear wave was 94 mm. The directivity of the shear wave was constant during the propagation. Refracted angle differences between the nominal angle and measured angle in the test probe are due to the small velocity differences between steel and the glass model.

Figure 6 shows the center of directivity of shear waves in 2- and 4-MHz angle

probes. The centers of directivity were located behind the incident point and inside of the probe, and were not changed during the wave propagation.

Directivity of Reflected Shear Wave from Slit Defect in a Simulated Butt Joint

Figure 7A shows the visualized image of the shear wave reflected from the slit defect, having a propagation distance of 20 mm from the center point of directivity. The frequency of the angle probe was 4 MHz. A probe was put on the left side of the defect (far defect), as shown in Fig. 3. The incident wave was propagated from the upper left-hand to the bottom right-hand side, as shown in the diagram. Four reflected shear waves are observed in the visualized image.

Figure 7B shows the directivity obtained from Fig. 7A. The angle of the reflected shear waves numbered 1, 2 and 3 were 65, 28 and 78 deg, respectively. In the case of the number 4 shear wave, the propagate direction agrees almost with the direction of number 2, but the intensity of the reflection wave was very weak compared with that of number 2. The directivity of the number 4 reflection wave was expressed superimposed in the directivity of number 2. This means the directivity of the four reflected shear waves were expressed with the three-directivity peak because of the direction and intensity of reflected shear waves.

Figure 8 shows the change of directivity due to the probe forward movement. The angle probe was moved forward from the maximum echo position to the –6 dB echo position. The angles of the reflected shear waves were 25, 63 and 78 deg, almost the same as in Fig. 7.

Figure 9 shows the change of directivity due to the probe's backward movement. Four shear waves reflected from the defect can be seen in Fig. 9A. The pattern of directivity was largely changed. To investigate the reason for this, we measured the directivity of each reflected shear wave. Figure 9C shows the directivity of wave numbers 1 and 2. Figure 9D shows the directivity of numbers 3 and 4. The angle of each reflection wave agrees with the results of Figs. 7B and 8. This means the propagate direction of the reflected shear waves was not changed with the probe position, but the intensity of each directivity was changed with the probe position.

Figure 10 shows the visualized image and the directivity of 2-MHz, 60-deg shear waves reflected from the defect. The angle of the reflection wave was 64 deg, almost the same as the angle of the incident wave. The directivity pattern is quite different from the result given by 4-

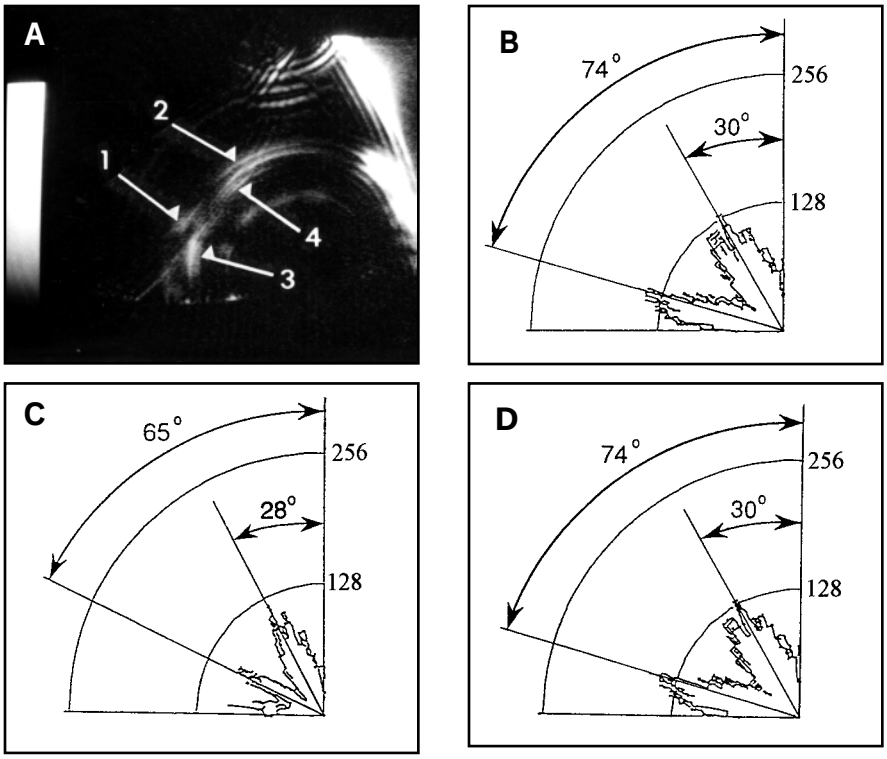

Fig. 9 — Change of directivity by probe backward movement (4 MHz, 60 deg). A — Visualized shear waves (R = 12 mm); B — directivity of reflected all-shear waves; C — directivity of number 1 and 2 waves; D — directivity of number 3 and 4 waves.

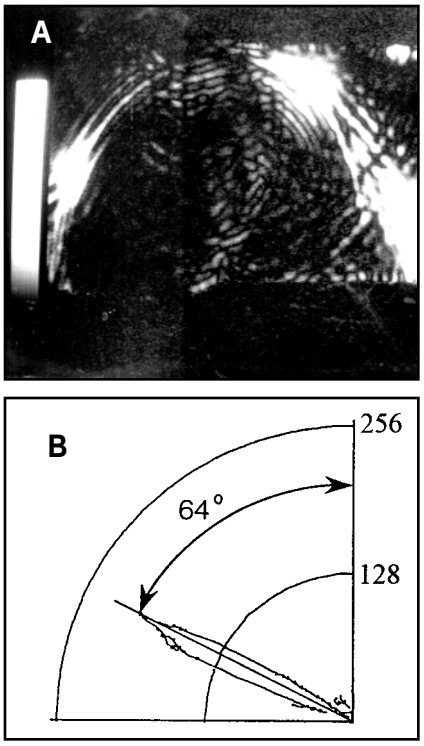

Fig. 10 — Directivity of 2-MHz, 60-deg shear waves reflected from far defect. (Probe was at the maximum echo position.) A — Visualized shear waves (R = 20 mm); B — directivity of reflected shear waves.

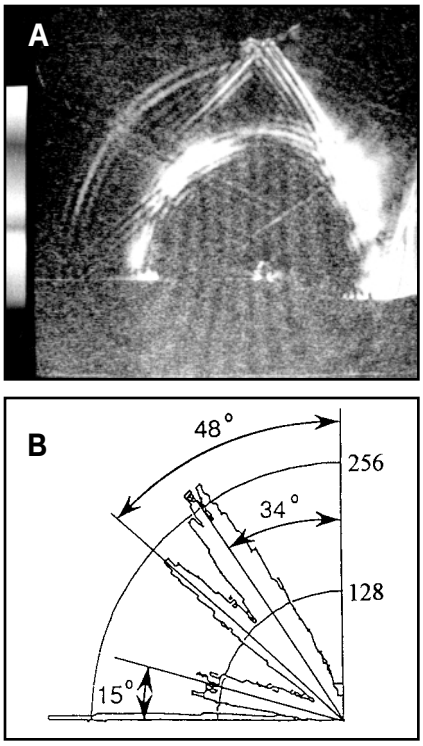

Fig. 11 — Directivity of 4-MHz, 60-deg shear waves reflected from near defect. (Probe was at the maximum echo position). A — Visualized shear waves (R = 12 mm); B — directivity of reflected shear waves.

MHz angle probes. With the 2-MHz angle probe, the measured defect size decreased compared with that of the 4-MHz angle probe because the wavelength of the 2-MHz shear wave (1.7 mm) is twice as long as the 4-MHz shear wave (0.85 mm).

Figure 11 shows the visualized image and the directivity of the 4-MHz, 60-deg shear waves. The probe was put on the right side of the centerline (near defect) of the simulated butt joint (Fig. 3) at the maximum echo position. The angles of the reflection waves were 34, 48 and 75 deg. The directivity of reflected shear waves was changed with the incident direction of ultrasonic to the defect (far defect, near defect).

Conclusions

This article studies the directivity of ultrasonic waves emitted from the angle probes and reflected from the defect in a simulated weld joint by the visualization method.

The directivity of shear waves emitted from the angle probes was constant during the propagation. The center of directivity was almost constant and was located inside of the angle probes. The directivity of shear waves reflected from the slit defect were different according to probe direction (far defect, near defect), probe position (forward movement, maximum echo position, backward movement), but the intensity of each directivity was changed with the probe position. A difference of directivity of the reflection wave existed between 2- and 4-MHz angle probes. With the 2-MHz angle probe, the directivity appeared sharp because of the relation of the wavelength and defect size. The above results can be applied to the choice of probe arrangement, correct measurement of defect size and location in ultrasonic testing of metals (steel, iron).

Acknowledgment

The author wishes to thank Prof. K. Date of Tohoku University (Japan) for useful discussions.

References

1. *Nondestructive Testing Handbook*, Vol. 7. 1991. ASNT, Columbus, Ohio, pp. 551–566.

2. KrautKramer, J., and KrautKramer, H. 1990. Ultrasonic testing of materials, *Springer-Verlag*, pp. 58–92.

3. Ludwig, R., and Lord, W. 1986. Development in the finite element modeling of ultrasonic NDT phenomena. *Review of Progress in Quantitative Nondestructive Evaluation* 5A: 73–81.

4. Ogilvy, J. A. 1986. Theoretical comparison of ultrasonic signal amplitudes from smooth and rough defects. *NDT International*, December, pp. 371–385.

5. Ogilvy, J. A. 1986. Ultrasonic beam profiles and beam propagation in an austenitic weld using a theoretical ray tracing model. *Ultrasonic*, November, pp. 337–347.

6. Ogilvy, J. A. 1987. On the use of focused beams in austenitic welds. *British Journal of NDT*, July, pp. 238–246.

7. You, Z., and Lord, W. 1989. Finite element study of elastic wave interaction with cracks. *Review of Progress in Quantitative Nondestructive Evaluation* 8A: 109–116.

8. Ogilvy, J. A. 1992. An interactive ray tracing model for ultrasonic nondestructive testing. *NDT International*, February, pp. 3–10.

9. Harumi, K. 1986. Computer simulation of ultrasonic in a solid. *Material Evaluation* 44: 1086–1114.

10. Hall, K. G. 1977. A qualitative evaluation of variable-angle ultrasonic transducers by the photoelastic visualization method. *Ultrasonics*, November, pp. 245–252.

11. Hall, K. G. 1982. Observing ultrasonic wave propagation by stroboscopic visualization method. *Ultrasonics*, July, pp. 159–167.

12. Hall, K. G. Visualization technique for the study of ultrasonic wave propagation in the railway industry. *Materials Evaluation*, June, pp. 922–929.

13. Date, K., Tabata, Y., and Shimada, H. 1987. A quantitative evaluation of ultrasonic wave in solid by the photoelastic visualization method. IEEE Ultrasonic Symposium, pp. 1093–1097.

14. Date, K., and Udagawa, Y. 1989. Visualization of ultrasonic waves in a solid by stroboscopic photoelasticity and image processing techniques. *Review of Progress in Quantitative Nondestructive Evaluation* 8B: 1755–1762.

15. Nam, Y. H., and Date, K. 1995. Directivity analysis of angle probes and surface defects by ultrasonic visualization method. *Review of Progress in Quantitative Nondestructive Evaluation* 14: 1091–1098.